

BRIEF REPORT

The recurrent postzygotic pathogenic variant p.Glu47Lys in *RHOA* causes a novel recognizable neuroectodermal phenotype

Gökhan Yigit^{1*} | Ken Saida^{2*} | Danielle DeMarzo³ | Noriko Miyake²  |
 Atsushi Fujita² | Tiong Yang Tan^{4,5} | Susan M. White^{4,5} | Alexandra Wadley³ |
 Mohammad R. Toliat⁶ | Susanne Motameny⁶ | Marek Franitza⁶ | Chloe A. Stutterd^{4,5} |
 Pin F. Chong⁷ | Ryutaro Kira⁷ | Toru Sengoku⁸  | Kazuhiro Ogata⁸ |
 Maria J. Guillen Sacoto⁹ | Christine Fresen¹⁰ | Bodo B. Beck^{11,12,13} |
 Peter Nürnberg^{6,12} | Christoph Dieterich¹⁴ | Bernd Wollnik^{1,15}  |
 Naomichi Matsumoto^{2*} | Janine Altmüller^{6,12*} 

¹Institute of Human Genetics, University Medical Center Göttingen, Göttingen, Germany

²Department of Human Genetics, Graduate School of Medicine, Yokohama City University, Yokohama, Japan

³University of Oklahoma Health Sciences Center, Oklahoma City, Oklahoma

⁴Victorian Clinical Genetics Services, Murdoch Children's Research Institute, Melbourne, Australia

⁵Department of Paediatrics, University of Melbourne, Melbourne, Australia

⁶Cologne Center for Genomics, University of Cologne, Cologne, Germany

⁷Department of Pediatric Neurology, Fukuoka Children's Hospital, Fukuoka, Japan

⁸Department of Biochemistry, Graduate School of Medicine, Yokohama City University, Yokohama, Japan

⁹GeneDx, Gaithersburg, Maryland

¹⁰Department of Psychosomatics and Psychotherapy, University Hospital Cologne, Cologne, Germany

¹¹Institute of Human Genetics, University Hospital Cologne, Cologne, Germany

¹²Center for Molecular Medicine Cologne (CMMC), University of Cologne, Cologne, Germany

¹³Center for Rare Diseases Cologne (ZSEK), University of Cologne, Cologne, Germany

¹⁴Department of Internal Medicine III, Partner Site Heidelberg/Mannheim, DZHK (German Centre for Cardiovascular Research), University Hospital Heidelberg, Heidelberg, Germany

¹⁵Cluster of Excellence "Multiscale Bioimaging: from Molecular Machines to Networks of Excitable Cells" (MBExC), University of Göttingen, Göttingen, Germany

Correspondence

Gökhan Yigit, Institute of Human Genetics,
 University Medical Center Göttingen, Heinrich-
 Dürer-Weg 12, 37073 Göttingen, Germany.
 Email: goekhan.yigit@med.uni-goettingen.de

Janine Altmüller, Cologne Center for Genomics,
 University of Cologne, Weyertal 115b 50931
 Cologne, Germany.
 Email: janine.altmueller@uni-koeln.de

Abstract

RHOA is a member of the Rho family of GTPases that are involved in fundamental cellular processes including cell adhesion, migration, and proliferation. RHOA can stimulate the formation of stress fibers and focal adhesions and is a key regulator of actomyosin dynamics in various tissues. In a Genematcher-facilitated collaboration, we were able to identify four unrelated individuals with a specific phenotype characterized by hypopigmented areas of the skin, dental anomalies, body asymmetry, and limb length discrepancy

*Gökhan Yigit, Ken Saida, Naomichi Matsumoto, and Janine Altmüller contributed equally to this work.

This is an open access article under the terms of the Creative Commons Attribution-NonCommercial License, which permits use, distribution and reproduction in any medium, provided the original work is properly cited and is not used for commercial purposes.

© 2019 The Authors. *Human Mutation* published by Wiley Periodicals, Inc.

Funding information

AMED, Grant/Award Numbers: JP18kk020501, JP19dm0107090, JP19ek0109280, JP19ek0109301, JP19ek0109348; Deutsche Forschungsgemeinschaft, Grant/Award Numbers: AL901/2-1, AL901/3-1, EXC 2067/1-390729940, KFO 329; JSPS, Grant/Award Numbers: JP17H01539, JP19H03621; Takeda Science Foundation; Ministry of Health, Labour and Welfare

due to hemihypotrophy of one half of the body, as well as brain magnetic resonance imaging (MRI) anomalies. Using whole-exome and ultra-deep amplicon sequencing and comparing genomic data of affected and unaffected areas of the skin, we discovered that all four individuals carried the identical *RHOA* missense variant, c.139G>A; p.Glu47Lys, in a postzygotic state. Molecular modeling and in silico analysis of the affected p.Glu47Lys residue in *RHOA* indicated that this exchange is predicted to specifically alter the interaction of *RHOA* with its downstream effectors containing a PKN-type binding domain and thereby disrupts its ability to activate signaling. Our findings indicate that the recurrent postzygotic *RHOA* missense variant p.Glu47Lys causes a specific mosaic disorder in humans.

KEYWORDS

hemihypotrophy, postzygotic mutations, *RHOA*, skin hypopigmentation, small GTPases

The GTPases of the Rho family were initially discovered due to their homology to Ras GTPases (Madaule & Axel, 1985). To date, approximately 20 Rho GTPases have been described in mammals, and are important mediators of signaling pathways linking extracellular signals to cytoskeletal changes, thereby regulating fundamental cellular processes including cell adhesion, cell migration, and proliferation (Etienne-Manneville & Hall, 2002; Olson, Ashworth, & Hall, 1995; Yamamoto et al., 1993). Rho family GTPases are molecular switches, which cycle between an inactive guanosine diphosphate- (GDP)-bound form and an active guanosine triphosphate- (GTP)-bound form. The activity of Rho GTPases is further controlled by cellular factors including guanine nucleotide-exchange factors, GTPase-activating proteins, and guanine nucleotide-dissociation inhibitors, which are all capable of regulating the cycling of Rho GTPases between the active and inactive states (Heasman & Ridley, 2008; Vetter & Wittinghofer, 2001). *RHOA* is a member of the Rho family of GTPases that stimulates the formation of stress fibers and focal adhesions and is, therefore, a key regulator of actomyosin dynamics in various tissues (Chrzanowska-Wodnicka & Burridge, 1996; Nobes & Hall, 1995; Ridley & Hall, 1992). In contrast to *RhoB* and *RhoC*, its closest homologs within the family of Rho GTPases, *RhoA*-null mice have not been reported. Conditional, tissue-specific deletion of *RhoA* demonstrates its physiological role during neural development, apoptosis in the postnatal neocortex, and in the regulation of skin cell proliferation and differentiation (Herzog et al., 2011; Katayama et al., 2011; McMullan et al., 2003; Sanno et al., 2010). In humans, germline pathogenic variants in *RHOA* have not been described. Unlike for Ras family GTPases, for a long time, somatic mutations in cancer were only very rarely reported for Rho family GTPases including *RHOA*. Today, due to advances in sequencing technologies, recurrent somatic mutations in *RHOA*, for example, in angioimmunoblastic T-cell lymphoma, adult T-cell leukemia/lymphoma as well as in diffuse-type gastric cancer and other solid tumors were revealed (Kakiuchi et al., 2014; Palomero et al., 2014; Sakata-Yanagimoto et al., 2014; Yoo et al., 2014).

In this study, we identified somatic mosaicism for a recurrent *RHOA* variant in four unrelated individuals with overlapping clinical features. We

used the GeneMatcher (Sobreira, Schiettecatte, Valle, & Hamosh, 2015) tool to connect the three centers at the University Hospital Cologne (University of Cologne, Cologne, Germany), the Graduate School of Medicine (Yokohama City University, Yokohama, Japan) and the University of Oklahoma Health Sciences Center (Oklahoma City, OK), in which clinical examination of patients and/or genetic analyses took place, and we were able to show by next-generation sequencing (NGS) approaches that all four individuals carry the identical missense variant, c.139G>A; p.Glu47Lys, in the Rho family GTPase *RHOA* (MIM# 165390; RefSeq NM_001664.4). Molecular modeling and in silico analysis of the affected amino acid indicated that this exchange might alter the interaction of *RHOA* with its downstream effectors and thereby disrupt its ability to activate signaling.

All four individuals reported herein are born to nonconsanguineous families and are not related to each other. Subjects or their legal representatives gave written informed consent, and all studies were performed in accordance with the Declaration of Helsinki protocols. The studies were reviewed and approved by the local institutional ethics board (University Hospital Cologne, University of Cologne; the Graduate School of Medicine, Yokohama City University; University of Oklahoma Health Sciences Center).

Individual 1 is a 35-year-old female of German origin. She was born at term by uncomplicated spontaneous delivery as the first child of healthy nonconsanguineous parents after an uneventful pregnancy. Her birth weight was 2,900 g (−0.9 standard deviation [SD]), her birth length was 49 cm (−0.9 SD; Table 1). During growth, asymmetry was noted involving limbs, feet, teeth, and the whole body including mild affection of the face, which resulted in a right-sided hemihypotrophy. Additionally, an abdominal ultrasound revealed the size differences of the kidneys (right < left). Acral anomalies included brachydactyly and broad left first toe (Figure 1a). Genome-wide chromosomal analysis (karyotype and array-Comparative-Genomic-Hybridization), as well as genetic testing for Silver-Russel syndrome (SRS; MIM# 180860), produced normal results. Hypopigmentation of the skin was observed most prominently on the right lower leg and was following the lines of Blaschko. Additionally, a

TABLE 1 Clinical features of affected individuals

	Individual 1	Individual 2	Individual 3	Individual 4
Age (years)	35	10	12	3
Sex	Female	Female	Female	Female
Birth				
Gestation (weeks)	40	39	38	39
Weight (g)	2,900 (−0.9 SD)	3,360 (−0.2 SD)	2,562 (−0.7 SD)	2,410
Length (cm)	49 (−0.9 SD)	48 (−0.5 SD)	49 (−0.5 SD)	46
Head circumference (cm)	NR	34 (−0.5 SD)	32 (−0.7 SD)	NR
Clinical Characteristics				
Depigmentation of skin	Yes	Yes, UV-sensitivity	Yes	Yes
Facial dysmorphism	Yes, mild asymmetry	Yes, prominent forehead, facial asymmetry, short palpebral fissures, a square jaw with micrognathia, malar flattening, short philtrum, small mouth and dysplastic, squared ears	No	Yes, posterior auricular prominent forehead, relative macrocephaly, triangular shaped face, micrognathia, small mouth
Ocular anomalies	Yes, bilateral myopia and astigmatism	Yes, congenital glaucoma left and right, hypoplasia of the left optic nerve	No	Yes, vision loss, differentially sized eyes
Hearing loss	No	Yes, bilateral high-frequency sensorineural hearing loss	No	Yes, unilateral (right-sided) sensorineural hearing loss
Hair abnormality	Yes, hypopigmented streaks	Yes, focal alopecia	No	Yes, thin brittle hair
Dental anomalies	Yes, asymmetric microdontia	Yes, oligodontia, misshapen teeth, and dental caries	Yes, anomalies of the right incisor	No
Body/limb asymmetry	Yes, right-sided hemihypotrophy	Yes, right-sided hemihypotrophy	Yes, left-sided hemihypotrophy	Yes, left-sided hemihypotrophy
Acral anomalies	Yes, brachydactyly, broad left first toe	Yes, syndactyly, long great toes, overlapping toes	Yes, syndactyly	No
Seizures	No	Yes, focal clonic seizures	No	No
Brain MRI anomalies	Yes, multifocal white matter lesions, lesion of the brainstem, small cerebellar lesions	Yes, periventricular and deep lobar white matter anomalies, multiple small cysts	Yes, multicystic periventricular white matter lesions of the right lateral ventricles	Yes, generalized ventricular dilation and periventricular leukomalacia, pituitary hypoplasia
Current measurements				
Height (cm)	154 (−2.1 SD)	136.7 (−0.2 SD)	147 (−1.1 SD)	93.4
Development	Normal	Difficulties in reading and writing mainly related to hearing and vision impairment	Normal	Global developmental, delay behavioral abnormalities

Abbreviations: NR, not recorded; SD, standard deviation; UV, ultraviolet.

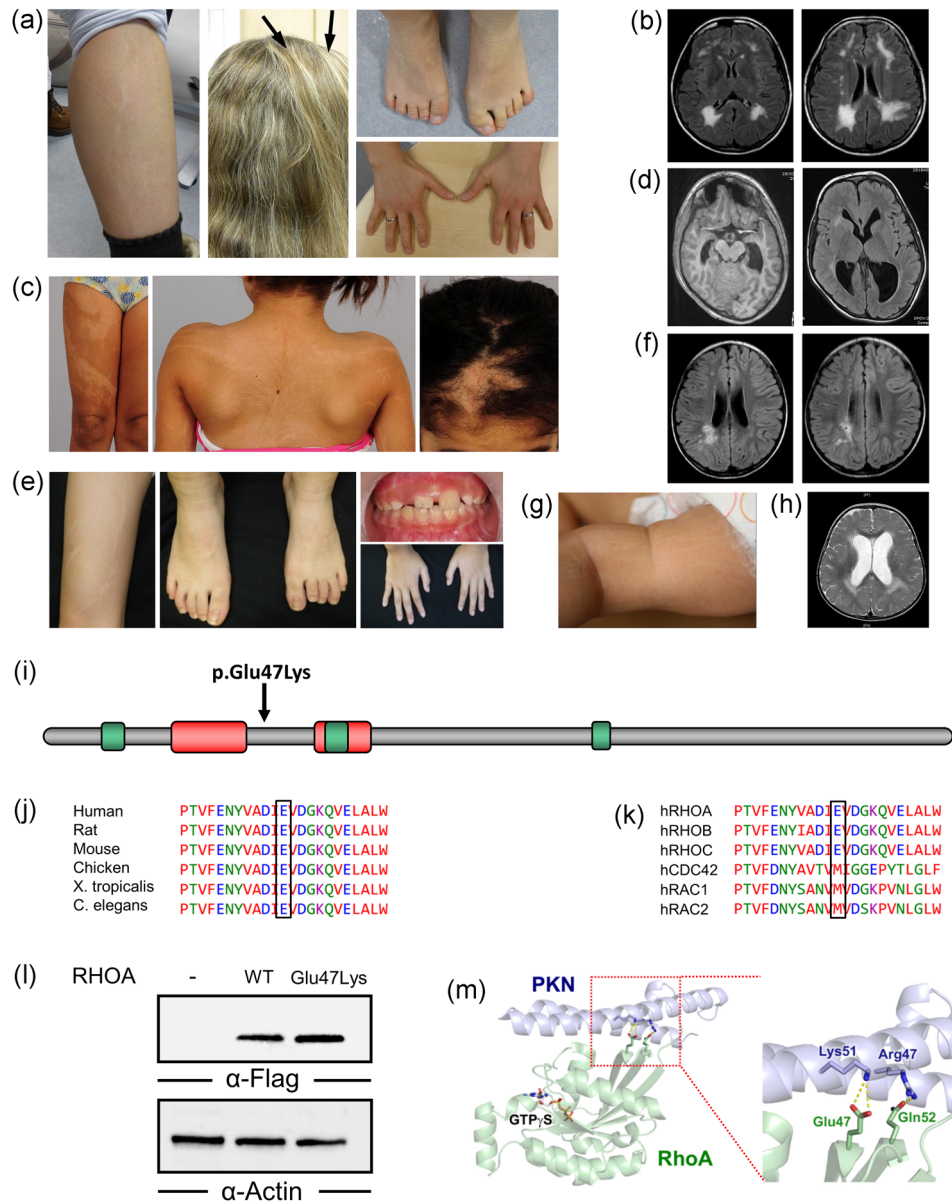


FIGURE 1 Clinical characteristics of individuals harboring a recurrent somatic mosaicism in RHOA and in silico and functional analysis of the identified RHOA variant p.Glu47Lys shown are Individual 1 (a, b), Individual 2 (c, d), Individual 3 (e, f), and Individual 4 (g, h). Shared physical features include hypopigmentation of the skin, length discrepancy affecting hands and feet, and limb anomalies including brachydactyly and syndactyly. Hypopigmented streaks in Individual 1 are indicated by black arrow (a). Brain MRI of Individual 1 (b), Individual 2 (d), Individual 3 (f), and Individual 4 (h) showing multifocal white matter lesions, a lesion of the brainstem (b), abnormalities of the periventricular and deep lobar white matter (d), and white matter lesions with multiple cystic changes (f). (i) Representation of full-length human RHOA protein (RefSeq NM_001664.4; Uniprot: P61586). The relative position of the pathogenetic variant identified in all three individuals is indicated by the arrow. Regions involved in GTP/GDP binding are depicted as green boxes, red boxes represent switch regions of hRHOA. Conservation of the p.Glu47 residue across different species (j) and among selected members of the Rho family GTPases (k). Protein sequences were prepared from UniProt (<https://www.uniprot.org>) and alignment was performed using Clustal Omega (<https://www.ebi.ac.uk/Tools/msa/clustalo>). Black boxes indicate the position of the RHOA p.Glu47 amino acid. (l) HEK293T cells were transiently transfected either with an RHOA wild-type or mutant (Glu47Lys) expression vector, or left untransfected as control (-). Immunoblot analysis was performed with FLAG antibodies (upper panel), and equal protein loading was confirmed by reprobng the membrane with anti- β -actin antibodies (lower panel). The western blots were performed in triplicate. (m) Structure of the GTP-bound form of RHOA complexed with the effector domain of PKN. Structural information were obtained from the Protein Data Bank (www.rcsb.org/pdb) and are available under the accession number 1XZ. RHOA and PKN are colored green and purple, respectively, in complex with GTP_γS, a nonhydrolysable analog of GTP (left picture). A close-up view of the RHOA p.Glu47 residue and its nearby residues (right picture). Hydrophilic interactions of RHOA residues with PKN are shown as yellow dotted lines

streak of depigmentation was observed on the right side of her scalp hair (Figure 1a). Right-sided microdontia was noted. Brain magnetic resonance imaging (MRI) during adolescence and adulthood revealed multifocal white matter lesions, a lesion of the brainstem and small cerebellar lesions (Figure 1b). Her cognitive and motor development was normal. Her height is currently 154 cm (-2.1 SD), and she has a 2 years old healthy daughter.

Individual 2 is a 10-year-old female of Greek-Australian ancestry born as the second child to nonconsanguineous healthy parents. Her pregnancy was complicated by the detection of pyelectasis at 19 weeks gestation and ventriculomegaly at 32 weeks gestation. Chromosomal analysis of cultured amniocytes obtained by amniocentesis showed a normal female karyotype. Her birth weight was 3,360 g (-0.2 SD), her birth length 48 cm (-0.5 SD), and her head circumference 34 cm (-0.5 SD; Table 1). She presented with right-sided hemihypotrophy. Facial dysmorphism included a prominent forehead, large anterior fontanelle, facial asymmetry, short palpebral fissures, a square jaw with micrognathia, malar flattening, short philtrum, small mouth and dysplastic, squared ears. We observed an unusual anterior hairline with a region of alopecia in the scalp hair (Figure 1c). She had mild bilateral high-frequency hearing loss currently not requiring the use of hearing aids, and ophthalmology assessment identified bilateral anterior segment dysgenesis with glaucoma and cataract. An ocular prosthesis was implanted into the right eye, and she had cataract extraction, an intra-ocular lens replacement, and placement of a tube shunt at her left eye. She undergoes persistent glaucoma treatment with oral and topical therapies. She had complete syndactyly of the right third and fourth fingers (Figure 1c) and was diagnosed with a moderately sized muscular ventricular septal defect. Renal ultrasound was normal. She had feeding difficulties requiring nasogastric feeding in the first year of life. By age 20 months, she developed mixed hypo- and hyperpigmentation of the skin along Blaschko's lines on upper and lower limbs, with hypopigmented areas hypersensitive to ultraviolet light. Some primary and permanent dentition were missing and teeth that were present were small, misshapen and had developed caries. Her scalp hair was sparse and showed progressive patchy alopecia (Figure 1c). At 2 years of age, she developed focal clonic seizures which mostly occurred from sleep. No anticonvulsants were prescribed and she has had no seizure recurrence since the age of eight. MRI of the brain showed abnormalities of the periventricular and deep lobar white matter in keeping with diffuse periventricular leukoencephalopathy, and we observed abnormal signals within the basal ganglia and thalami indicating multiple small cysts (Figure 1d). Her current global development at the age of 10 years is borderline to normal and mainly affected due to difficulties in reading and writing related to her hearing and vision impairment. She attends mainstream school with support. Her current height is 136.7 cm (-0.2 SD), and she has a 3 cm leg-length discrepancy.

Individual 3 is a 12-year-old female of Japanese ancestry born as the second child of healthy nonconsanguineous parents after 38 weeks of gestation. Her birth weight was 2,562 g (-0.7 SD) and the head circumference was 32.0 cm (-0.7 SD; Table 1). She presented with acral anomalies including syndactyly of the 2nd and 3rd toes of her left foot which was surgically corrected at the age of

two (Figure 1e). Further, left-sided hemihypotrophy was observed. After sustaining an accidental head trauma at the age of four, brain MRI revealed multicystic periventricular white matter lesions of the right lateral ventricles which were confirmed at a follow-up MRI at 11 years, revealing the slight progression of the observed lesions (Figure 1f). Upon clinical examination, she presented with hypopigmented whorled lesions at the upper left (shoulder including upper arm) and lower left (buttocks to knee) extremities, following Blaschko's lines (Figure 1e). Further examination revealed anomalies of one permanent tooth (right incisor). Hearing impairment or eye anomalies were not identified. Cognitive and motor development was normal. Chromosomal analysis revealed a normal female karyotype (46, XX). Her current height is 147 cm (-1.1 SD).

Individual 4 is a 3-year-old female of Native American and German ancestry. She was born after 39 weeks of gestation via cesarean section. During pregnancy, the ultrasound revealed renal cysts. Prenatal chromosomal analysis showed a normal female karyotype. Her birth weight was 2,410 g, her birth length 46 cm. At the age of 2 months, left-sided hemihypotrophy and the leg-length discrepancy were detected. She presented with facial dysmorphic features including relative macrocephaly, triangular-shaped face, prominent ears, posterior auricular prominent forehead, micrognathia, a small mouth, and she had thin brittle hair (Figure 1g). She failed newborn hearing screening and was diagnosed with right-sided sensorineural hearing loss. Brain MRI which was performed due to hypotonia showed large ventricles, leukomalacia, and a small pituitary (Figure 1h). She had a dysplastic left kidney, renal function of the right kidney was normal. The endocrine evaluation showed no abnormalities and she had normal blood pressure. No cardiac issues were detected. She developed skin anomalies including hyper- and hypopigmented patches that were following the lines of Blaschko, and pathological analysis of a skin biopsy of the affected area was consistent with epidermal nevi. Genetic testing for imprinting disorders was negative as well as testing for SRS. An SNP array was performed which gave normal results showing only two regions of homozygosity on Xq22.2q23 and 5q14.3. She had feeding difficulties leading to feeding via a PEG tube. Weight gain was normal. Currently, she shows a global development delay and has difficulties with expressive language. Hearing aids are applied, and she gets speech and occupational therapy on a weekly base.

As the clinical features in all four individuals suggested genetic mosaicism, our analysis focused on genomic data from nonblood tissues. We performed whole-exome sequencing (WES) on DNA extracted from a buccal swab from the left side of Individual 1 and compared the results to WES data generated from DNA, which was isolated from a skin biopsy of the right lower leg within a clearly visible line of hypopigmentation of the same individual. DNA isolation was carried out following standard protocols and WES was performed as previously described (Altmüller et al., 2016). WES data analysis and filtering of variants were carried out using the exome and genome analysis pipeline "Varbank" (<https://varbank.ccg.uni-koeln.de>) of the Cologne Center for Genomics (University of Cologne) and we obtained a mean coverage of 95 and 96 reads,

and 88.4% and 89.6% of exome targets were covered at least 30 \times , respectively. WES data were filtered for variants with coverage of >30 reads, a minimum quality score of 10, and an allele frequency (AF) \geq 10%. Using the integrated DeNovoGear software (Ramu et al., 2013), which allows the pair-wise analysis of exome datasets, we identified only a single variant that differed between both samples. This variant, c.139G>A, was located in exon 2 of the *RHOA* gene and it was present at an AF of 24% (12 of 51 total reads) in DNA extracted from the skin biopsy of Individual 1, whereas it was completely absent in DNA from buccal swab of the same individual (0 of 64 reads). Furthermore, we could confirm the *RHOA* c.139G>A variant by PCR and subsequent Sanger sequencing on DNA from the skin biopsy of Individual 1 (Figure S1). In Individual 2, targeted gene panel sequencing of an MTOR related in-house panel covering 268 genes including *RHOA* was performed as previously described (Fujita et al., 2019) on DNA derived from fibroblast obtained by skin biopsy. We obtained a mean coverage of 767 for all coding bases and splice junctions. Data were analyzed for somatic variants, which uncovered a single variant, *RHOA* c.139G>A, that was present in a mosaic state at an AF of 6.1% (58 of 955 reads). Similar to Individual 1, WES using DNA extracted from blood and a skin biopsy was performed in Individual 3. Somatic variant calling was performed with VarScan2 and MuTect2 (Cibulskis et al., 2013; Koboldt et al., 2012). We identified the variant c.139G>A in *RHOA* in a mosaic state in eight out of 27 reads (AF of 29.6%) in DNA extracted from the skin biopsy of Individual 3, whereas it was absent in DNA from the blood of the same individual (0 of 37 reads). In Individual 4, WES was performed on DNA extracted from blood and a skin biopsy of the affected individual as described previously (Retterer et al., 2016). Whereas we were not able to identify the c.139G>A variant in *RHOA* in DNA from the blood (0 of 98 reads) of Individual 4, it was present in 24 out of 54 reads in DNA extracted from the skin biopsy (AF of 40.7%) indicating genetic mosaicism of the identified variant.

The c.139G>A variant in *RHOA*, which we detected in all four individuals, is not observed in any current database of human genetic variations including the ExAC (<http://exac.broadinstitute.org>) and gnomAD (<https://gnomad.broadinstitute.org>) database (access date 27/11/2019; Karczewski et al., 2019; Lek et al., 2016). It is predicted to lead to the substitution of a phylogenetically highly conserved glutamate at the amino acid position 47 of *RHOA* by lysine (p.Glu47Lys; Figure 1i–k). In silico prediction modelling using different prediction tools lead to consistent variant classification of damaging (SIFT; <https://sift.bii.a-star.edu.sg>; prediction score: 0.012; cutoff: 0.05), probably damaging (PolyPhen-2; <http://genetics.bwh.harvard.edu/pph2>; HumDiv score: 0.997), disease-causing (MutationTaster; <http://www.mutationtaster.org>), and a CADD (<https://cadd.gs.washington.edu>) score of 33, respectively, indicating deleteriousness of this variant. Similarly to its Rho GTPase family members RAC1 and CDC42, *RHOA* is a highly conserved protein that is under strict mutational constraint. For the canonical transcript of *RHOA* (ENST00000418115.1; <https://www.ensembl.org>) only 13 missense variants were reported in the gnomAD database in contrast to 114 that were expected to be observed in the >140,000 exomes and genomes ($z = 3.36$).

To further determine the AF of this variant, we used an NGS-based deep sequencing approach on DNA from skin samples from each individual. In Individual 1, we found that the c.139G>A variant had an AF of 11% in an unaffected area of the lower left leg, and 14% and 28% at >200k fold coverage in two skin biopsies independently taken from hypopigmented, affected areas of the lower right leg. Samples taken from affected tissue of Individuals 2 and 3 had an AF of 8.3% at >100k fold coverage and 25.6% at >10k fold coverage, respectively. Notably, we detected the c.139G>A variant neither in DNA from a buccal swab or blood-derived from Individual 1, nor in DNA from the blood of Individual 3 (Tables S1–S3). Next, we analyzed DNA extracted from parental saliva samples of Individual 2 and parental blood samples of Individual 3. We found that the c.139G>A variant had an AF of 0% at >80k fold coverage and >100k fold coverage, respectively, in the mother and father of Individual 2, and an AF of 0% at 9k fold coverage and >10k fold coverage in the mother and father of Individual 3, respectively (Tables S2 and S3).

To analyze the effect of the p.Glu47Lys variant on *RHOA* protein stability, we cloned wild-type (WT) and mutant *RHOA* complementary DNA (cDNA) into a mammalian expression vector and tagged both with an N-terminal FLAG tag. Transfection of HEK293T cells with both WT and mutant *RHOA* and subsequent Western blot analysis revealed comparable steady-state expression levels of both WT and mutant *RHOA* proteins indicating that the p.Glu47Lys variant in *RHOA* does not have any impact on *RHOA* protein stability (Figure 1l).

To gain further insights into the pathogenic effects of the *RHOA* missense variant, we then modeled the p.(Glu47Lys) substitution on the crystal structure of the GTP-bound form of RhoA complexed with the effector domain of protein kinase N1 (PKN1; Maesaki et al., 1999). p.Glu47 is highly conserved across species and within the Rho family members (Figure 1j,k). It is located in a three-stranded beta-sheet on the surface of the protein, which allows its interaction with RhoA-binding partners. As the p.Glu47 is located distant from the GTP binding site, the p.Glu47Lys substitution is unlikely to affect the conformational stability or the GTP binding or -hydrolysis activities of RhoA. Instead, we modeled that p.Glu47 mediates the interaction with PKN1, a protein kinase C-related serine/threonine kinase that can be activated by *RHOA* and thereby regulates diverse cellular processes such as cytoskeletal changes, cell adhesion, and vesicle transport (Amano et al., 1996; Mukai, 2003). The PKN1 effector domain contains three alpha-helices, two of which are assembled into a coiled-coil structure and involved in multiple interactions with *RHOA*. At the interaction interface, two *RHOA* residues (p.Glu47 and p.Gln52) are located close to each other and form hydrophilic interactions with two basic residues of PKN1, p.Lys51, and p.Arg47, respectively (Figure 1m). The *RHOA* p.Glu47Lys substitution does not only disrupt the ionic interaction with the PKN1 p.Lys51, but also generates an electrostatic repulsion with the two basic residues of PKN1. The *RHOA* residues p.Glu47 and p.Gln52 are highly conserved only among the Rho-like subfamily members *RHOA*, *RHOB*, and *RHOC*, but not in other related small GTPase proteins including RAC1 and CDC42, which highlights the importance of the interactions observed in the complex structure for specific functions of *RHOA* (Figure 1j,k). Several *RHOA*-specific effector proteins contain a basic residue

(Lys or Arg) corresponding to PKN1 p.Lys51, suggesting a common mechanism of RHOA interaction and binding (Bishop & Hall, 2000; Maesaki et al., 1999). Thus, p.(Glu47Lys) substitution, which we identified in all four affected individuals, may directly affect the binding ability of RHOA to its downstream effectors that contain a PKN-type interaction domain and may thereby lead to compromised RHOA signaling.

In this report, we provide evidence that the RHOA variant c.139G>A causes a distinct phenotype comprising hypopigmentation of the skin, dental anomalies, body asymmetry, and brain MRI anomalies. Remarkably, all four individuals carry the identical RHOA c.139G>A variant in a postzygotic state.

The c.139G>A; p.(Glu47Lys) RHOA variant affects a functionally important residue. This variant has been detected in 13 of 66,223 unique samples within the COSMIC (Catalogue of Somatic Mutations in Cancer; <https://cancer.sanger.ac.uk/cosmic>) database in samples from cancer of the urinary tract (9), pleura (1), skin (1), soft tissue (1), and the upper aerodigestive tract (1; Tate et al., 2019). Still, it is a rather rare variant of RHOA observed in cancer. Most frequently, mutations of p.Gly17 in RHOA are detected in cancer samples. This mutation affects a highly conserved residue that is involved in GTP binding, and functional analyses have revealed that it disrupts GTP binding and thereby acts in a dominant-negative way regarding stress fiber formation and transcriptional activation (Palomero et al., 2014; Sakata-Yanagimoto et al., 2014; Yoo et al., 2014). Interestingly, the mutated guanine nucleotide at position 139 is part of a CpG site. Methylation of cytosines at these sites has been associated with high mutation rates, as spontaneously occurring deamination of methylated cytosine results in thymine. Due to the palindromic methylation pattern, which often is observed at CpG sites, this might explain the detection of this specific variant in all of our patients.

Currently, we can only speculate about the functional effects of the RHOA p.(Glu47Lys) variant, which is located within the effector domain of RHOA. Using structural modeling we showed that this variant affects a residue that is directly involved in binding of the serine/threonine PKN1, a downstream target of activated RHOA. As additional RHOA effectors containing a PKN-type domain are known, including PRK2, rhotekin, and rhophilin, the effect of the mutation might not be limited to compromised effector signaling via PKN1 (Bishop & Hall, 2000; Maesaki et al., 1999). Functional analyses of different residues in the RHOA effector domain indicate that specific disruption of RHOA-PKN1 interaction has an impact on actin stress fiber formation (Sahai, Alberts, & Treisman, 1998). This could also be the case for the p.Glu47Lys variant and might point to a possible dominant-negative effect of the variant. Additionally, Rho family GTPases have also been shown to be involved in the transcriptional regulation of a huge variety of cellular factors. In combination with the serum response factor, RHOA can activate gene transcription from c-fos serum response elements and can initiate PKN1-dependent signaling events leading to activation of extracellular signal-regulated kinase 6 and thereby regulating gene expression and cellular processes (Hill, Wynne, & Treisman, 1995; Marinissen, Chiariello, & Gutkind, 2001). However; further experimental studies will be needed to address this possibility and to determine potential disease-causing mechanisms of the identified p.Glu47Lys variant in RHOA.

We were unable to identify the c.139G>A variant in DNA derived from blood lymphocytes even with ultra-deep sequencing with up to >200k fold coverage in all four individuals. This might indicate that the presence of the variant could be disadvantageous for the cells and that, therefore, cells carrying the variant are underrepresented or even eliminated especially in highly proliferating tissue as it was shown for different genetic disorders caused by mosaic mutation including, for example, Proteus syndrome (Lindhurst et al., 2011). Additionally, we observed different variant allele frequencies during culturing of skin-derived fibroblasts of 14% measured on genomic DNA in the initial skin biopsy, and 10% after 30 days of culturing, as measured by ultra-deep sequencing of a PCR-derived amplicon on cDNA derived from cultured fibroblasts. It has been shown that RHOA is involved in cell cycle regulation and cell proliferation (Villalonga, Villalonga, & Ridley, 2006). Therefore, reduction of the number of mutated cells might be caused by altered and slower cell proliferation compared to cells harboring two WT RHOA alleles, or indicate lower expression levels of the mutated c.139G>A allele.

The role of Rho family GTPases during brain development has been intensively studied. Patients carrying heterozygous mutations in Rho family members RAC1, RAC3, and CDC42 present with multiple brain MRI abnormalities such as hypoplasia of the corpus callosum and cerebellar vermis, enlarged ventricles, and periventricular white matter lesions (Costain et al., 2019; Martinelli et al., 2018; Reijnders et al., 2017). Targeted deletions of *RhoA* in spinal cord neuroepithelium, midbrain, and forebrain of mice showed an impact on cell polarity and cell-cell junctions (Herzog et al., 2011; Katayama et al., 2011). Interestingly, RhoA also seems to be an important regulator of cell survival and proliferation of neuronal progenitor cells as shown by functional studies of dominant-negative mutants of RhoA (Numano et al., 2009). The deletion of *RhoA* in the cerebral cortex of mice revealed a crucial role of RhoA for neuronal migration in the developing cerebral cortex (Cappello et al., 2012). Similarly to affected individuals described here, these mice presented with a thinner cerebral cortex, and detailed analyses revealed that the neuronal migration defects were not caused by RhoA activity in migrating neurons themselves, but were due to alterations and destabilization of the actin and microtubule cytoskeleton of the radial glia scaffold, which is crucial for directing migrating neurons.

Very recently, mutations in RHOA have been associated with the mosaic neuroectodermal syndrome (Vabres et al., 2019). In six of seven patients presenting with hypopigmentation, facial and acral anomalies, and brain MRI abnormalities Vabres et al. (2019) identified the identical missense mutation p.Glu47Lys in RHOA. Interestingly, they observed a facial asymmetry in all affected patients, whereas body asymmetry, which in our study was present in all cases, was only reported in 2/7 patients.

In conclusion, we show that the recurrent postzygotic missense variant p.Glu47Lys in RHOA causes a specific human phenotype characterized by hypopigmentation of the skin, dental anomalies, body asymmetry, and length discrepancy of limbs, as well as brain MRI anomalies. In our study, all four individuals carry the identified variation as a somatic mosaic variant, suggesting that, in contrast to,

for example, other Rho family members like RAC1, RAC3, and CDC42 (Costain et al., 2019; Martinelli et al., 2018; Reijnders et al., 2017), nonmosaic mutations in RHOA might be lethal, and we speculate that the distinct phenotype observed in our patients is caused by disruption of RHOA interaction with its effectors.

ACKNOWLEDGMENTS

We are grateful to all family members that participated in this study, Luise Graichen, Elisabeth Kirst, and Ramona Caspar for excellent technical assistance, and Karin Boss for critically reading the manuscript. Furthermore, we thank the Regional Computing Center of the University of Cologne (RRZK) for providing computing time on the Deutsche Forschungsgemeinschaft (DFG) funded high-performance computing system CHEOPS as well as support. This work was supported by AMED to N. Matsumoto; JSPS KAKENHI to N. Matsumoto and to N. Miyake; grants from the Ministry of Health, Labor, and Welfare to N. Matsumoto; grants from the Takeda Science Foundation to N. Matsumoto and N. Miyake; the DFG (German Research Foundation) under Germany's Excellence Strategy to B. Wollnik; the DFG (German Research Foundation)—Clinical research unit to J. Altmüller. This work was supported by the Japan Agency for Medical Research and Development (AMED), grant/award numbers: JP19ek0109280, JP19dm0107090, JP19ek0109301, JP19ek0109348, and JP18kk020501; Japan Society for the Promotion of Science (JSPS) KAKENHI, grant/award numbers: JP17H01539 and JP19H03621; Deutsche Forschungsgemeinschaft (DFG; German Research Foundation) under Germany's Excellence Strategy, grant/award number: EXC 2067/1-390729940; DFG (German Research Foundation), grant/award numbers: KFO 329, AL901/2-1, and AL901/3-1.

CONFLICT OF INTERESTS

Maria J. Guillen Sacoto is an employee of GeneDx, Inc. The authors declare that there are no conflict of interests.

DATA AVAILABILITY STATEMENT

The data that support the findings of this study are available on request from the corresponding author. The genetic data are not publicly available due to privacy or ethical restrictions.

ORCID

Noriko Miyake  <http://orcid.org/0000-0003-0987-310X>
 Toru Sengoku  <http://orcid.org/0000-0001-9461-8714>
 Bernd Wollnik  <http://orcid.org/0000-0003-2589-0364>
 Janine Altmüller  <http://orcid.org/0000-0003-4372-1521>

REFERENCES

- Altmüller, J., Motameny, S., Becker, C., Thiele, H., Chatterjee, S., Wollnik, B., & Nürnberg, P. (2016). A systematic comparison of two new releases of exome sequencing products: The aim of use determines the choice of product. *Biological Chemistry*, 397(8), 791–801. <https://doi.org/10.1515/hsz-2015-0300>
- Amano, M., Mukai, H., Ono, Y., Chihara, K., Matsui, T., Hamajima, Y., ... Kaibuchi, K. (1996). Identification of a putative target for Rho as the serine-threonine kinase protein kinase N. *Science (New York, NY)*, 271(5249), 648–650. <https://doi.org/10.1126/science.271.5249.648>
- Bishop, A. L., & Hall, A. (2000). Rho GTPases and their effector proteins. *The Biochemical Journal*, 348(Pt 2), 241–255.
- Cappello, S., Böhringer, C. R. J., Bergami, M., Conzelmann, K.-K., Ghanem, A., Tomassy, G. S., ... Götz, M. (2012). A radial glia-specific role of RhoA in double cortex formation. *Neuron*, 73(5), 911–924. <https://doi.org/10.1016/j.neuron.2011.12.030>
- Chrzanowska-Wodnicka, M., & Burridge, K. (1996). Rho-stimulated contractility drives the formation of stress fibers and focal adhesions. *The Journal of Cell Biology*, 133(6), 1403–1415. <https://doi.org/10.1083/jcb.133.6.1403>
- Cibulskis, K., Lawrence, M. S., Carter, S. L., Sivachenko, A., Jaffe, D., Sougnez, C., ... Getz, G. (2013). Sensitive detection of somatic point mutations in impure and heterogeneous cancer samples. *Nature Biotechnology*, 31(3), 213–219. <https://doi.org/10.1038/nbt.2514>
- Costain, G., Callewaert, B., Gabriel, H., Tan, T. Y., Walker, S., Christodoulou, J., ... Meyn, M. S. (2019). De novo missense variants in RAC3 cause a novel neurodevelopmental syndrome. *Genetics in Medicine: Official Journal of the American College of Medical Genetics*, 21(4), 1021–1026. <https://doi.org/10.1038/s41436-018-0323-y>
- Etienne-Manneville, S., & Hall, A. (2002). Rho GTPases in cell biology. *Nature*, 420(6916), 629–635. <https://doi.org/10.1038/nature01148>
- Fujita, A., Higashijima, T., Shirozu, H., Masuda, H., Sonoda, M., Tohyama, J., ... Matsumoto, N. (2019). Pathogenic variants of DYNC2H1, KIAA0556, and PTPN11 associated with hypothalamic hamartoma. *Neurology*, 93, e237–e251. <https://doi.org/10.1212/WNL.00000000000007774>
- Heasman, S. J., & Ridley, A. J. (2008). Mammalian Rho GTPases: New insights into their functions from in vivo studies. *Nature Reviews Molecular Cell Biology*, 9(9), 690–701. <https://doi.org/10.1038/nrm2476>
- Herzog, D., Loetscher, P., van Hengel, J., Knüsel, S., Brakebusch, C., Taylor, V., ... Relvas, J. B. (2011). The small GTPase RhoA is required to maintain spinal cord neuroepithelium organization and the neural stem cell pool. *The Journal of Neuroscience: The Official Journal of the Society for Neuroscience*, 31(13), 5120–5130. <https://doi.org/10.1523/JNEUROSCI.4807-10.2011>
- Hill, C. S., Wynne, J., & Treisman, R. (1995). The Rho family GTPases RhoA, Rac1, and CDC42Hs regulate transcriptional activation by SRF. *Cell*, 81(7), 1159–1170.
- Kakiuchi, M., Nishizawa, T., Ueda, H., Gotoh, K., Tanaka, A., Hayashi, A., ... Ishikawa, S. (2014). Recurrent gain-of-function mutations of RHOA in diffuse-type gastric carcinoma. *Nature Genetics*, 46(6), 583–587. <https://doi.org/10.1038/ng.2984>
- Karczewski, K. J., Francioli, L. C., Tiao, G., Cummings, B. B., Alföldi, J., Wang, Q., ... MacArthur, D. G. (2019). Variation across 141,456 human exomes and genomes reveals the spectrum of loss-of-function intolerance across human protein-coding genes. *BioRxiv*, 531210. <https://doi.org/10.1101/531210>
- Katayama, K., Melendez, J., Baumann, J. M., Leslie, J. R., Chauhan, B. K., Nemkul, N., ... Yoshida, Y. (2011). Loss of RhoA in neural progenitor cells causes the disruption of adherens junctions and hyperproliferation. *Proceedings of the National Academy of Sciences of the United States of America*, 108(18), 7607–7612. <https://doi.org/10.1073/pnas.1101347108>

- Koboldt, D. C., Zhang, Q., Larson, D. E., Shen, D., McLellan, M. D., Lin, L., ... Wilson, R. K. (2012). VarScan 2: Somatic mutation and copy number alteration discovery in cancer by exome sequencing. *Genome Research*, 22(3), 568–576. <https://doi.org/10.1101/gr.129684.111>
- Lek, M., Karczewski, K. J., Minikel, E. V., Samocha, K. E., Banks, E., & Fennell, T., ... Exome Aggregation Consortium. (2016). Analysis of protein-coding genetic variation in 60,706 humans. *Nature*, 536(7616), 285–291. <https://doi.org/10.1038/nature19057>
- Lindhurst, M. J., Sapp, J. C., Teer, J. K., Johnston, J. J., Finn, E. M., Peters, K., ... Biesecker, L. G. (2011). A mosaic activating mutation in AKT1 associated with the proteus syndrome. *New England Journal of Medicine*, 365(7), 611–619. <https://doi.org/10.1056/NEJMoa1104017>
- Madaule, P., & Axel, R. (1985). A novel ras-related gene family. *Cell*, 41(1), 31–40.
- Maesaki, R., Ihara, K., Shimizu, T., Kuroda, S., Kaibuchi, K., & Hakoshima, T. (1999). The structural basis of Rho effector recognition revealed by the crystal structure of human RhoA complexed with the effector domain of PKN/PRK1. *Molecular Cell*, 4(5), 793–803.
- Marinissen, M. J., Chiariello, M., & Gutkind, J. S. (2001). Regulation of gene expression by the small GTPase Rho through the ERK6 (p38 gamma) MAP kinase pathway. *Genes & Development*, 15(5), 535–553. <https://doi.org/10.1101/gad.855801>
- Martinelli, S., Krumbach, O. H. F., Pantaleoni, F., Coppola, S., Amin, E., Pannone, L., ... Mirzaa, G. M. (2018). Functional dysregulation of CDC42 causes diverse developmental phenotypes. *American Journal of Human Genetics*, 102(2), 309–320. <https://doi.org/10.1016/j.ajhg.2017.12.015>
- McMullan, R., Lax, S., Robertson, V. H., Radford, D. J., Broad, S., Watt, F. M., ... Hotchin, N. A. (2003). Keratinocyte differentiation is regulated by the Rho and ROCK signaling pathway. *Current Biology: CB*, 13(24), 2185–2189.
- Mukai, H. (2003). The structure and function of PKN, a protein kinase having a catalytic domain homologous to that of PKC. *Journal of Biochemistry*, 133(1), 17–27. <https://doi.org/10.1093/jb/mvg019>
- Nobes, C. D., & Hall, A. (1995). Rho, rac, and cdc42 GTPases regulate the assembly of multimolecular focal complexes associated with actin stress fibers, lamellipodia, and filopodia. *Cell*, 81(1), 53–62.
- Numano, F., Inoue, A., Enomoto, M., Shinomiya, K., Okawa, A., & Okabe, S. (2009). Critical involvement of Rho GTPase activity in the efficient transplantation of neural stem cells into the injured spinal cord. *Molecular Brain*, 2, 37. <https://doi.org/10.1186/1756-6606-2-37>
- Olson, M. F., Ashworth, A., & Hall, A. (1995). An essential role for Rho, Rac, and Cdc42 GTPases in cell cycle progression through G1. *Science (New York, NY)*, 269(5228), 1270–1272. <https://doi.org/10.1126/science.7652575>
- Palomero, T., Couronné, L., Khiabani, H., Kim, M.-Y., Ambesi-Impombato, A., Perez-Garcia, A., ... Ferrando, A. A. (2014). Recurrent mutations in epigenetic regulators, RHOA and FYN kinase in peripheral T cell lymphomas. *Nature Genetics*, 46(2), 166–170. <https://doi.org/10.1038/ng.2873>
- Ramu, A., Noordam, M. J., Schwartz, R. S., Wuster, A., Hurles, M. E., Cartwright, R. A., & Conrad, D. F. (2013). DeNovoGear: De novo indel and point mutation discovery and phasing. *Nature Methods*, 10(10), 985–987. <https://doi.org/10.1038/nmeth.2611>
- Reijnders, M. R. F., Anson, N. M., Kousi, M., Yue, W. W., Tan, P. L., Clarkson, K., ... Banka, S. (2017). RAC1 missense mutations in developmental disorders with diverse phenotypes. *American Journal of Human Genetics*, 101(3), 466–477. <https://doi.org/10.1016/j.ajhg.2017.08.007>
- Retterer, K., Juusola, J., Cho, M. T., Vitazka, P., Millan, F., Gibellini, F., ... Bale, S. (2016). Clinical application of whole-exome sequencing across clinical indications. *Genetics in Medicine*, 18(7), 696–704. <https://doi.org/10.1038/gim.2015.148>
- Ridley, A. J., & Hall, A. (1992). The small GTP-binding protein rho regulates the assembly of focal adhesions and actin stress fibers in response to growth factors. *Cell*, 70(3), 389–399.
- Sahai, E., Alberts, A. S., & Treisman, R. (1998). RhoA effector mutants reveal distinct effector pathways for cytoskeletal reorganization, SRF activation and transformation. *The EMBO Journal*, 17(5), 1350–1361. <https://doi.org/10.1093/emboj/17.5.1350>
- Sakata-Yanagimoto, M., Enami, T., Yoshida, K., Shiraishi, Y., Ishii, R., Miyake, Y., ... Chiba, S. (2014). Somatic RHOA mutation in angioimmunoblastic T cell lymphoma. *Nature Genetics*, 46(2), 171–175. <https://doi.org/10.1038/ng.2872>
- Sanno, H., Shen, X., Kuru, N., Bormuth, I., Bobsin, K., Gardner, H. A. R., ... Tucker, K. L. (2010). Control of postnatal apoptosis in the neocortex by RhoA-subfamily GTPases determines neuronal density. *The Journal of Neuroscience: The Official Journal of the Society for Neuroscience*, 30(12), 4221–4231. <https://doi.org/10.1523/JNEUROSCI.3318-09.2010>
- Sobreira, N., Schiettecatte, F., Valle, D., & Hamosh, A. (2015). GeneMatcher: A matching tool for connecting investigators with an interest in the same gene. *Human Mutation*, 36(10), 928–930. <https://doi.org/10.1002/humu.22844>
- Tate, J. G., Bamford, S., Jubb, H. C., Sondka, Z., Beare, D. M., Bindal, N., ... Forbes, S. A. (2019). COSMIC: The catalogue of somatic mutations in cancer. *Nucleic Acids Research*, 47(D1), D941–D947. <https://doi.org/10.1093/nar/gky1015>
- Vabres, P., Sorlin, A., Kholmanskikh, S. S., Demeer, B., St-Onge, J., Duffourd, Y., ... Rivière, J.-B. (2019). Postzygotic inactivating mutations of RHOA cause a mosaic neuroectodermal syndrome. *Nature Genetics*, 51(10), 1438–1441. <https://doi.org/10.1038/s41588-019-0498-4>
- Vetter, I. R., & Wittinghofer, A. (2001). The guanine nucleotide-binding switch in three dimensions. *Science (New York, NY)*, 294(5545), 1299–1304. <https://doi.org/10.1126/science.1062023>
- Villalonga, P., Villalonga, P., & Ridley, A. J. (2006). Rho GTPases and cell cycle control. *Growth Factors*, 24(3), 159–164. <https://doi.org/10.1080/08977190600560651>
- Yamamoto, M., Marui, N., Sakai, T., Morii, N., Kozaki, S., Ikai, K., ... Narumiya, S. (1993). ADP-ribosylation of the rhoA gene product by botulinum C3 exoenzyme causes Swiss 3T3 cells to accumulate in the G1 phase of the cell cycle. *Oncogene*, 8(6), 1449–1455.
- Yoo, H. Y., Sung, M. K., Lee, S. H., Kim, S., Lee, H., Park, S., ... Ko, Y. H. (2014). A recurrent inactivating mutation in RHOA GTPase in angioimmunoblastic T cell lymphoma. *Nature Genetics*, 46(4), 371–375. <https://doi.org/10.1038/ng.2916>

SUPPORTING INFORMATION

Additional supporting information may be found online in the Supporting Information section.

How to cite this article: Yigit G, Saida K, DeMarzo D, et al. The recurrent postzygotic pathogenic variant p.Glu47Lys in RHOA causes a novel recognizable neuroectodermal phenotype. *Human Mutation*. 2020;41:591–599. <https://doi.org/10.1002/humu.23964>